

Original Study

Open Access

Wiktor Sitek*, Agnieszka Kiersnowska, Vazgen Bagdasaryan, Eugeniusz Koda

The Impact of Different Strain Rates of Polypropylene Geotextiles on Slope Factor of Safety

<https://doi.org/10.2478/sgem-2025-0009>

received June 7, 2024; accepted December 20, 2024.

Abstract: Due to their effectiveness, environmental friendliness, and economic benefits, geosynthetics are increasingly utilized in civil engineering, especially woven geotextiles for soil stabilization reinforcement. Standard strength testing assumes a constant rate of elongation for samples, but in practice, the loading rate of geosynthetics in the field is much lower. Selecting appropriate materials is crucial for the effectiveness and durability of structures. For polymeric materials like woven geotextiles, the strain rate affects their properties. Understanding these properties is essential for safe design and construction. This article explores the potential application of polypropylene geotextiles for soil reinforcement in embankments. The polymer properties are discussed, along with the methodology for strength testing of geosynthetics and the results of the research. The findings allowed for the calculation of the long-term strength of samples at different elongation rates, which was used to verify changes in the factor of safety for a slope model. The highest tensile strength was 33.44 kN/m at a stretching speed of 20 mm/min. At 2 mm/min, it was 30.35 kN/m, and at 0.2 mm/min, it was 28.70 kN/m. These results determined the factor of safety: $F = 2.08$ for the fastest stretched sample and $F = 1.97$ for the slowest. Theoretical approaches to understanding changes in strength parameters due to variations in strain rate have been presented, as well as computational approaches using the Bishop method in GEO5 software, based on the results from tensile strength tests.

Keywords: Stability, Polypropylene Geotextile, Elongation Rate, Soil Stabilization, Factor of Safety

*Corresponding author: Wiktor Sitek, Warsaw University of Life Sciences – SGGW, Faculty of Civil and Environmental Engineering, ul. Nowoursynowska 159, 02-776 Warszawa, Poland, E-mail: wiktor_sitek@sggw.edu.pl

Agnieszka Kiersnowska, Vazgen Bagdasaryan, Eugeniusz Koda, Warsaw University of Life Sciences – SGGW, Faculty of Civil and Environmental Engineering, ul. Nowoursynowska 159, 02-776 Warszawa, Poland

1 Introduction

Modern manufacturing methods contribute to the improvement of mechanical, physical, and hydraulic properties of polymeric materials, including geosynthetics. These advantages enable their increasingly widespread use in engineering constructions. Reinforcing soil with woven geotextiles and related products can replace the conventional construction of retaining walls, rail and road embankments, as well as natural slopes as protecting systems against landslides (Benjamim et al., 2007; Yang et al., 2009; Duszyńska & Sikora, 2014; Koda et al., 2020; Dąbrowska et al., 2023). According to the EN ISO 10318 standard (ISO 10318-1:2015/Amd 1:2018), geosynthetics are defined as products in the form of strips, sheets, or three-dimensional forms with specified chemical, mechanical, and filtration properties. These products consist of at least one component made of polymer (such as polyester [PES], polypropylene [PP], polyethylene [PE], or polyamide [PA]). According to Table 1, geosynthetic fabrics are applied in various fields. Due to the production process and the materials used, they can fulfill most functions associated with geosynthetics. The chosen polymer and other additives give the material specific properties that make it suitable for use in construction applications.

Durability of geosynthetic materials is affected by endurance factors, related to the resistance of geosynthetics and impact of degradation factors, resulting from changes in the polymer at a molecular level (Greenwood, 2002; Kiersnowska et al., 2020; Paul & Pinho-Lopes, 2021). Endurance factors test their ability to withstand stresses like mechanical damage, creep, and abrasion. Degradation factors, such as ultraviolet (UV) radiation, high temperatures, and chemical exposure, can weaken the material over time. The significance of each factor depends on the specific project. Factors like site conditions, construction methods, and project timeline all play a role in determining which endurance and degradation factors will have the greatest impact on the geosynthetic's long-term performance (Greenwood et al., 2012; Hsuan et al., 2008; Kiersnowska et al., 2017).

Table 1: Functions of geosynthetics.

Type of geosynthetic	Filtration	Separation	Reinforcement	Sealing	Protection	Drainage	Barrier
Woven	X	X	X		X		
Nonwoven	X	X	X		X	X	
Geogrids			X				
Geonets		X	X				
Geocomposites			X	X		X	X
Geomembrane		X		X			X

Source: Shukla, Yin, 2006; Shukla, 2017; ISO 10318-1:2015/Amd 1:2018.

Geosynthetics reinforcing the soil can play a supportive role by not only increasing load-bearing capacity, but also simultaneously reducing deformations. Time-dependent stress–strain behavior is a crucial aspect of geosynthetics and needs careful consideration when designing structures. Geosynthetics, under constant load, can exhibit creep, meaning they continue to deform over time. This process can lead to excessive deflection or even failure in geotechnical construction not accounted for. However, due to constant strain, geosynthetics can experience stress relaxation, where the applied stress reduces over time, but the elongation remains unchanged. This can affect the overall performance and stability of the structure (Benjamim et al., 2007; Yang et al., 2009; Koda et al. 2020; Costa & Zornberg 2021).

In conclusion, the tensile response of geosynthetic materials is affected by several factors, including the type and arrangement of the polymer, environmental conditions, soil confinement, and loading level, rate, and duration.

The determination of tensile load capacity of polymeric reinforcements, particularly polyolefins like high-density polyethylene (HDPE) and PP, is challenging due to their rate-dependent mechanical behavior. This means the force required to break them and how much they stretch (tensile load–strain properties) depend on the speed of the pull (Allen & Bathurst 2002). For thermoplastic materials, the initial elastic deformation corresponds to that observed in metallic alloys and ceramic materials, associated with the elastic deformation of metallic, ionic, and covalent bonds between atoms. In addition, segments of entire polymer chains may undergo deformation (Dobrzański, 2002). Upon removal of stress, these segments gradually return to their original positions over time. Plastic deformation occurs when the yield point is exceeded, and involves stretching, untangling, displacing, and straightening of polymer chains under the influence of the load.

Initially, the chains may be more entangled and twisted, but they straighten as the stress increases (Dobrzański, 2002). At low temperatures and high deformation rates, thermoplastic polymer materials behave like other solid materials, including metals and ceramics. In the range of elastic deformation, there is a linear relationship between stress and strain. However, at elevated temperatures and low deformation rates, thermoplastic polymer materials behave like a viscous liquid. This polymer behavior explains their deformation under load (Dobrzański, 2002; Kiersnowska & Stępień, 2014). The tensile strength testing method according to EN ISO 10319 (ISO 10319:2015) specifies that the sample should be stretched at a constant rate of 20% per minute. In reality, the loading rate of reinforcement in the field during construction is orders of magnitude lower, typically five to six orders of magnitude lower (Lee & Lin, 2002). Standard laboratory test can lead to different mechanical properties if tests were performed at different strain rates (Ingold, 1994). It seems necessary to elaborate more rational design methods, which would be based on investigation of the influence of strain rate on the mechanical behavior of the material (Sawicki & Kazimierowicz-Frankowska, 2002). The selection of materials for geosynthetic reinforcement layers is essential to ensure the effectiveness and durability of the construction (Stępień & Szymański, 2015). In polymeric materials, the strain rate plays a crucial role because at higher strain rates, polymer molecular chains have less time for deformation, resulting in increased stiffness and apparent material strength (Stein, 2006).

Many civil engineering projects, especially large-scale ones such as dams, highways, and tunnels, face the common problem of slope subsidence. This serious phenomenon may lead to severe social and economic losses. To protect people and property, it is necessary to analyze the stability of excavation slopes, embankments, dams, and road embankments. Slope stability is largely

evaluated in light of the limit equilibrium method (LEM) (Bishop, 1955; Janbu, 1973; Morgenstern & Price, 1965).

In reality, during the construction of structures, more complex stress histories occur than during laboratory tests determining material strength, for example, loading at a constant strain rate followed by stress relaxation or creep, and then subsequent loading at a constant strain rate. Sawicki & Kazimierowicz postulated based on their tests that in such cases, the stress–strain curve is hardly affected by time-dependent phenomena (Sawicki & Kazimierowicz-Frankowska, 2002). Currently, in design practice, a creep reduction factor is applied, based on the creep-rupture curve obtained from tensile tests at a relatively high strain rate. The aim is to obtain the tensile strength at a specified design lifetime. Some available data indicate that the ultimate tensile strength of certain typical geosynthetics, obtained from loading tests conducted after prolonged creep tests, is not significantly lower than the value obtained from similar tests conducted at the same strain rate before the creep test (Hirakawa et al., 2002). The use of a creep reduction factor is implicitly based on the concept that creep is a degradation phenomenon for the tensile rupture strength of geosynthetics. This concept is seemingly linked to the description of time-dependent strength and deformation characteristics of geosynthetics by the isochronous concept. According to the isochronous concept, the current stress of a given geosynthetic reinforcement is a unique function of the instantaneous strain that has developed and the time that has elapsed since the start of loading (Hirakawa et al., 2002; Hirakawa et al., 2003). However, there is also the possibility of simulating the load–strain curve through appropriate computational approaches. The common load–strain characteristic can be represented by the following parabolic empirical equation:

$$\sigma = C\varepsilon^2 \tag{1}$$

where σ = force per unit width (designated in the subsequent sections as stress), ε = classical strain, and C = constant. Equation 1 is valid only in the range of loading up to the yield point (Sawicki & Kazimierowicz-Frankowska, 2002).

Hirakawa et al. (2002) emphasize that the deformation and ultimate tensile strength of geosynthetics primarily depend on the immediate rate of irreversible deformation, irrespective of the duration since loading initiation. This suggests that creep is not a degradation phenomenon like chemical or weathering processes. As a result, there is no necessity to incorporate a creep adjustment factor when evaluating the design tensile strength, though it should

be specified for the design strain rate. They also highlight that the isochronous model notably underestimates the tensile strength of geosynthetic reinforcement under relatively fast loading conditions. Furthermore, they highlight the effectiveness of the three-component model, a nonlinear rheology model, in accurately simulating the stress–strain response of geological materials exposed to various stress histories. According to this model, stress is decomposed as follows for the monotonic loading case:

$$\sigma = \sigma^f(\varepsilon^{ir}) + \sigma^v(\varepsilon^{ir}, \dot{\varepsilon}^{ir}, h_s) \tag{2}$$

where $\sigma^f(\varepsilon^{ir})$ is the inviscid stress component that is a unique function of the instantaneous irreversible strain ε^{ir} , while $\sigma^v(\varepsilon^{ir}, \dot{\varepsilon}^{ir}, h_s)$ is the viscous stress that is a function of ε^{ir} its rate $\dot{\varepsilon}^{ir}$, and the stress history parameter h_s .

This model was originally developed for geomaterials and then modified for geosynthetic reinforcement without changing its basic structure and features (Kongkitul et al., 2014). The model comprises three components, labeled as E, P, and V. According to the model, regardless of the specific properties of these three components, the total tensile load (T) consists of the inviscid tensile load (T^f) and the viscous tensile load (T^v), while the total strain rate ($\dot{\varepsilon}$) is decomposed into the elastic strain rate ($\dot{\varepsilon}^e$) and the irreversible (i.e., visco-plastic) strain rate ($\dot{\varepsilon}^{ir}$).

$$T = T^f + T^v \tag{3}$$

$$\dot{\varepsilon} = \dot{\varepsilon}^e + \dot{\varepsilon}^{ir} \tag{4}$$

A notable characteristic of the model is that removing the nonlinear viscous component, V, transforms it into a nonlinear elasto-plastic model. Further removal of the nonlinear plastic component results in a hypoelastic model. Hence, any existing elastic or elasto-plastic model can seamlessly transition to this nonlinear three-component model (Kongkitul et al., 2014).

Similar studies focused on the improvement of soil using geosynthetics can be found in the literature. Hassan et al. (2022) conducted research on shear strength behavior and a numerical study on geosynthetic-reinforced cohesive soil slopes. They performed triaxial compression tests, where the influence of geosynthetics was examined. Their results showed that the inclusion of reinforcement improved soil stiffness, friction angle, apparent cohesion, and shear strength. Similar to this study, they used computational software to determine the slope factor of safety, utilizing both finite element method (FEM) and LEM. Using Slide, Slope/W, and PLAXIS 2D software, they found that the factor of safety increased

with the rise in the amount of geosynthetic reinforcement (Hassan et al., 2022). However, the different strain rate, which is crucial during the installation of geosynthetics, was not considered in their research.

Similarly, Stępień and Szymański (2015) conducted a comparable study. However, they focused on the simultaneous effect of temperature and strain rate. Their results indicate an increase in the tensile strength of geotextile with the increase in strain rate. According to the information presented earlier, this relationship is also maintained at higher temperatures, although not as high as at standard temperature, as they demonstrated. However, this study lacks the use of the obtained information for calculations to verify how these results relate to the application of geotextiles in reinforcement functions. Most sources discussing the issue of using geosynthetics in soil present methods of testing them, for example, through triaxial compression (Hassan, 2023), which is undoubtedly effective. However, these tests are limited by the equipment and sample dimensions, which may affect the results.

The research described in this article allowed for the calculation of the long-term strength of samples at different strain rates, which was then used to verify changes in the stability coefficient of a slope model. Tensile strength tests accurately determined the tensile strength of PP geotextiles. Data from laboratory tests were used in calculations, enabling an assessment of the real impact of strain rate on slope safety factors. These studies contribute to a better understanding of the behavior of geotextiles under different load conditions and, over time, could be integrated into guidelines for designing reinforcement structures after further research on other materials.

2 Materials

The material subjected to laboratory testing was PP geotextile. The aim of the test was to examine how the tested material would respond to changes in the strain rate, and then with the results, check the factor of safety on the slope model. The majority of geotextiles are produced from PP or PET (Shukla & Yin, 2006). PP is a crystalline thermoplastic polymer obtained through the polymerization of propylene monomer in the presence of the stereospecific Ziegler–Natta catalyst system. Homopolymers are used for the production of fibers and threads, while copolymers find applications in various industrial fields. PP consists solely of hydrocarbons and

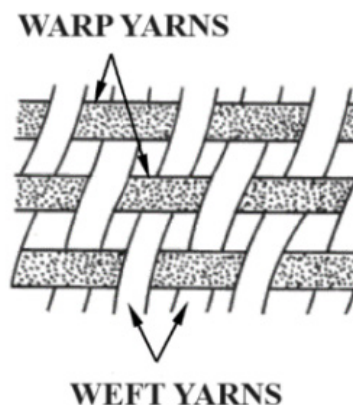


Figure 1: Plain weave geotextile (Shukla, 2017).

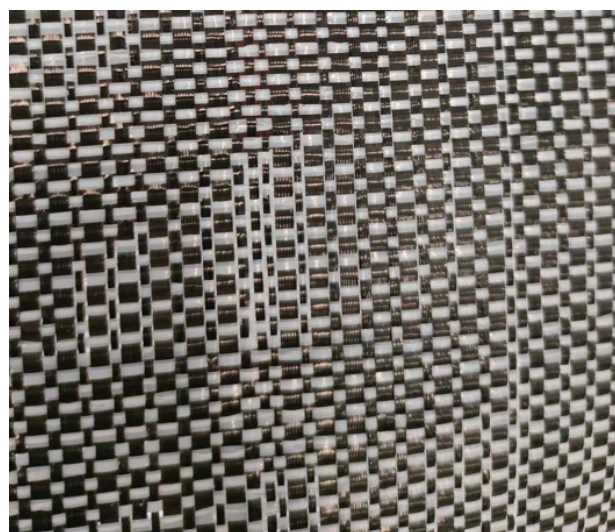


Figure 2: Geotextile subjected to testing (own photography).

is chemically inert (Agrawal, 2011). PP is characterized by high strength and stiffness (Miszkowska, 2015). Geotextiles are formed in a process similar to weaving clothing (Agrawal, 2011). They have a distinctive arrangement of two sets of parallel thread strands. The warp is the thread running along the length, and the weft is the one perpendicular to it (Shukla, 2017).

There are various types of weaves in geotextiles, but the most commonly encountered is the plain weave, depicted in Figure 1. In this weave, the weft threads pass alternately over and under the warp threads, creating a simple cross pattern (Koerner, 2012), which is also visible in Figure 2 which shows the geotextile subjected to test.

Table 2. presents the product parameters provided by the manufacturer, with strength testing conducted according to the EN ISO 10319 standard (ISO 10319:2015).

Table 2: Parameters of the geotextile subjected to testing.

Tensile strength		Maximum elongation at load		Static puncture resistance	Dynamic puncture resistance	Thickness	Unit mass	Pore size characteristics
Length-wise	Width-wise	Length-wise	Width-wise	4.3 kN	8.3 mm	0.37 mm	200 g/m ²	190 μm
32 kN/m	32 kN/m	18%	14%					

Source: manufacturer’s data

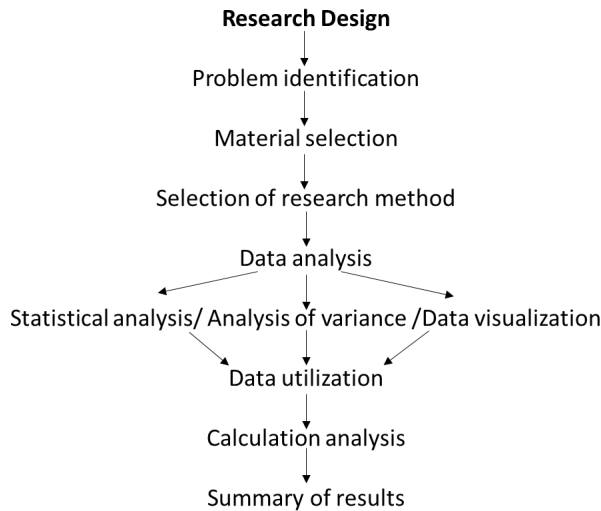


Figure 3: Flowchart of the research process.

3 Methodology

The study was designed according to Figure 3. For the strength testing using the wide-width strip method, five samples of geotextile were prepared for each series. The dimensions of the samples were 200 mm in width and 200 mm in length, with a length of 100 mm between the jaws of the testing machine. The remaining part of the geotextile sample allowed for its secure attachment to the machine jaws. According to EN ISO 9862, the samples were cut from a roll, with the external layers being removed beforehand to ensure that any production defects would not affect the test results (ISO 9862:2007).

The current standard considers the service life of geotechnical structures to be 120 years. When designing reinforcement using geosynthetic materials, appropriate safety factors are applied to determine their long-term strength. Despite undeniable progress, there still remains a significant lack of consistency in the choice of standards and design methods, selection of safety factors, and variations in calculation programs. The most important

publication in Poland in this regard is the ITB Instruction 429/2008 (ITB, 2008), which regulates the principles of selecting reinforcement for retaining structures and steep slopes (Sobolewski & Ajdukiewicz, 2015). In this situation, we can rely on these guidelines as well as more detailed ones such as EBGeo (2011) or BS 8006:2010 (Sobolewski and Ajdukiewicz, 2015). To determine the long-term strength characteristics, the following relationships were used:

$$F_k = \frac{F_{o,k}}{A_1 * A_2 * A_3 * A_4} \tag{5}$$

where: F_k – long-term strength value of the geosynthetic; $F_{o,k}$ – short-term strength value of the geosynthetic; A_1 – the coefficient takes into account the deformation and damage during the creep of the reinforcement; it depends on the initial reinforcement material; A_2 – the coefficient takes into account the mechanical damage to the reinforcement during transport, placement, and compaction of the soil; A_3 – the coefficient takes into account the influence of connections; and A_4 – the coefficient takes into account the influence of the ground environment (ITB, 2008; Wysokiński & Kotlicki, 2008).

In the conducted study, an INSTRON tensile testing machine was used, with a maximum load capacity of 10 kN; in addition, an extensometer, capable of measuring the distance between two reference points on the specimen without damaging or slipping the sample, was used for geotextile testing. Testing machine and extensometer are presented in Figure 4. The data from the tensile testing machine and the extensometer were continuously transmitted to a computer with the appropriate software. This allowed the data to be collected in tables, enabling their interpretation.

The GEO5 program was used for Factor of Safety calculations. The chosen computational method was the Bishop method. The simplified Bishop method can be represented by the following equation:

Table 3: Compilation of tensile test results for the tested samples.

	20 mm/min		2 mm/min		0.2 mm/min	
	Tensile strength (kN/m)	Strain at maximum tensile strength (%)	Tensile strength (kN/m)	Strain at maximum tensile strength (%)	Tensile strength (kN/m)	Strain at maximum tensile strength (%)
1	30.00	5.70	29.35	6.60	28.70	10.30
2	31.20	5.70	30.35	7.00	27.45	9.00
3	31.05	5.20	28.20	6.60	27.15	9.10
4	33.44	5.60	29.20	7.30	27.15	9.30
5	32.25	5.60	29.90	6.70	26.70	9.30
Max value	33.44	5.70	30.35	7.30	28.70	10.30
Min value	30.00	5.20	28.20	6.60	26.70	9.00
Average value	31.55	5.60	29.40	6.80	27.45	9.40
Standard deviation	0.260	0.20	0.161	0.30	0.152	0.50

Source: own work

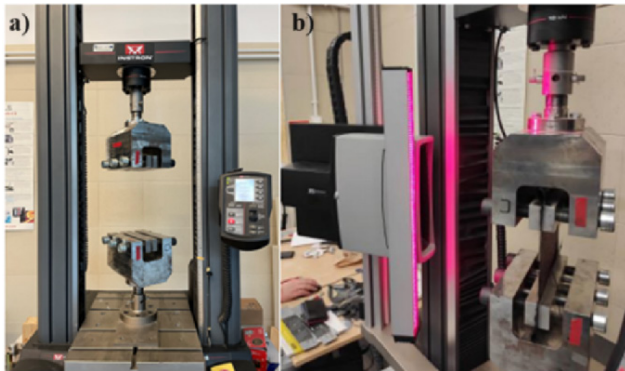


Figure 4: a) INSTRON tensile strength machine, b) extensometer (own photography).

$$F = \frac{\sum\{[c'b + (W - ub)tg\phi'] \frac{\sec\alpha}{1 + (tg\phi'tg\alpha/F)}\}}{\sum Wsina} \quad (6)$$

where: W – weight of the specimen (kN); b – width of the specimen (m); α – angle of inclination of the base of the specimen; u – water pressure in the pores (kN/m²); and ϕ' , c' – effective strength parameters of the soil (specifically, internal friction angle and cohesion) (Bishop, 1955).

The assumption of this method involves dividing the analyzed slope into computational blocks. The applied analysis method assumes potential loss of stability along the circular slip surface and takes into account the mutual interactions of forces acting between the jaws, which

become apparent in the limit equilibrium state (Koda et al., 2016).

4 Results

The test was conducted in four series, with each series consisting of five samples. The first three series comprised samples cut across the roll with stretching speeds of 20, 2, and 0.2 mm/min, while the remaining series consisted of samples cut along the roll with corresponding stretching speeds to the first three series. Due to the similarity of results and their time-consuming nature, it was decided to not continue the test for samples cut across the roller axis at speeds of 2 and 0.2 mm/min.

Based on the test results, it can be observed that the compilation of average values from each series indicates a decrease in the tensile strength of the material along with an increase in elongation values as the stretching velocity decreases. Specifically, for the sample stretched at a velocity of 2 mm/min, the tensile strength reduced by an average of 7% compared to the samples stretched at 20 mm/min. Similarly, the samples stretched at a velocity of 0.2 mm/min exhibited an average reduction of 14% in tensile strength compared to the samples stretched at 20 mm/min. Table 3 presents the results for the tensile testing of woven geotextile samples cut along the roller axis, including the compilation of maximum load and maximum deformation during maximum tensile strength.

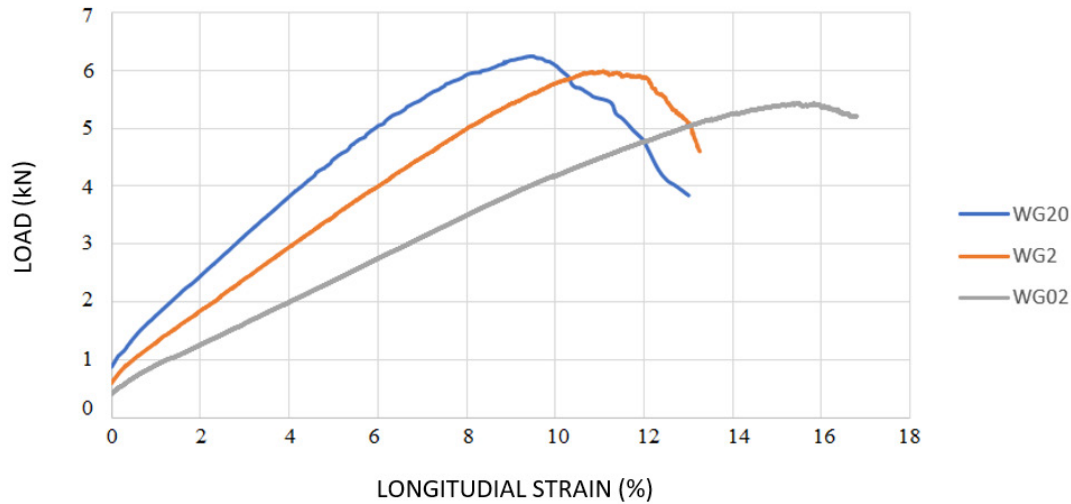


Figure 5: Comparison of typical results for different stretching speeds (own work).

Table 4: Reduction factors.

A1	A2	A3	A4
1.53	1.10	1.00	1.00

Source: ITB, 2008

Figure 5 presents a comparison of typical results for the tensile testing of a woven geotextile at different stretching speeds. It is noteworthy that there is a distinctive decrease in strength and an increase in deformation for samples stretched at speeds different from the norm, specifically WG2 – 2 mm/min and WG02 – 0.2 mm/min in this case.

Attention can also be given to the consistency of the test results. As mentioned earlier, all samples were prepared according to the standards. By excluding production-related defects and noting that all samples originated from the same roll and were stored in identical conditions, it can be concluded that the most consistent results, in terms of material strength, were obtained at a stretching speed of 0.2 mm/min. This indicates that the slower the stretching speed, the more uniform the material’s strength becomes.

The strain at maximum tensile strength of the tested samples increased as the velocity decreased. The slowest stretching sample had an average strain of 9.4%, while the fastest stretching sample had a strain of 5.6%. Based on the obtained results, the tensile strength for 1 m of the tested geotextile was determined as five times the value of the maximum tensile force (due to the width of the tested sample being 200 mm); therefore, $F_{o,k20} = 33.44$ kN/m, $F_{o,k2} = 30.35$ kN/m, and $F_{o,k02} = 28.72$ kN/m. The long-term

design strength F_k was also calculated based on Equation (1): $F_{k20} = 19.86$ kN/m, $F_{k2} = 18.03$ kN/m, and $F_{k02} = 17.06$ kN/m, assuming adopted reduction factors from Table 4.

5 Stability Analysis

To determine the safety factor and evaluate the influence of the PP geotextile on the stability of the structure, calculations were performed using the GEO5 software on the adopted computational model with the given soil parameters. The designed structure is a road embankment with a load of 20 kN/m², a height of 5 m, a crown width of 10 m, and a base width of 20 m. The slope inclination of the embankment is designed to be 1:2. The body of the embankment consists of medium sand (MSa), while the base is composed of silty clay (siCl) layer, according to Table 5.

In the initial calculation, the safety factor for the unreinforced slope was determined. The calculated value of the safety factor presented in Figure 6 is $F = 1.35$, which indicates that the allowable value of $F=1.5$ has not been achieved.

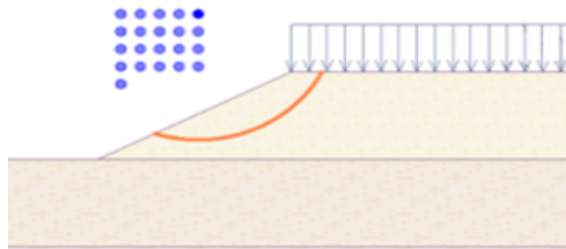
In the second case, four layers of PP geotextile were used for reinforcement. Each layer is placed at a distance of 1.25 m from the other layer, with a length of 10 m. The factor of safety for calculations using results for sample WG20 increased to a value of $F = 2.08$, which indicates that the structure can be considered safe (Fig. 7).

Figure 8 shows the calculation results for sample WG02. The factor of safety has once again reached a satisfactory value of $F = 1.97$. However, this value is lower than the

Table 5: Geotechnical parameters of soils.

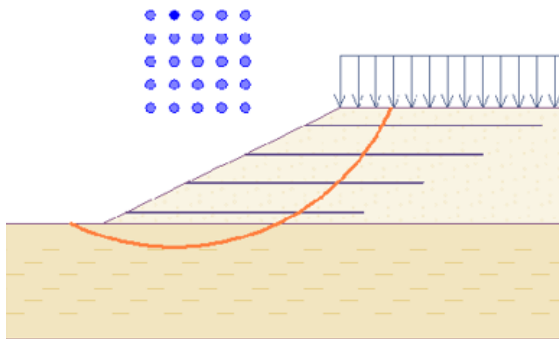
Type of soil	Thickness t (m)	Specific gravity γ (kN/m ³)	Dry density ρ_d (g/cm ³)	Angle of internal friction ϕ' (°)	Cohesion c' (kPa)
1. MSa	5	19	1.33	32	0
2. siCl	5	20	1.74	15	20

MSa: medium sand, siCl: silty clay



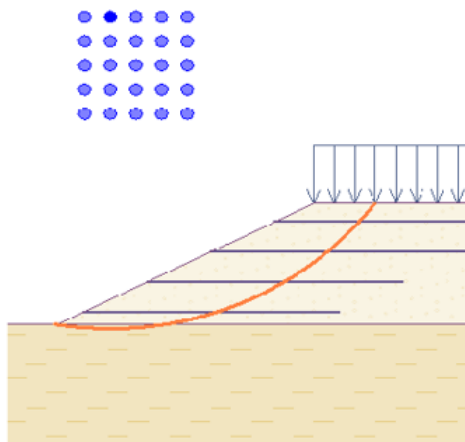
Sum of active forces : $F_a = 217.54$ kN/m
 Sum of passive forces : $F_p = 293.42$ kN/m
 Sliding moment : $M_a = 1566.12$ kN m/m
 Resisting moment : $M_p = 2112.41$ kN m/m
 Factor of safety = 1.35 < 1.50
Slope stability NOT ACCEPTABLE

Figure 6: Slip curves along with the obtained factor of safety (own work).



Sum of active forces : $F_a = 267.96$ kN/m
 Sum of passive forces : $F_p = 557.39$ kN/m
 Sliding moment : $M_a = 2679.63$ kN m/m
 Resisting moment : $M_p = 5573.91$ kN m/m
 Factor of safety = 2.08 < 1.50
Slope stability ACCEPTABLE

Figure 7: Slip curves along with the obtained factor of safety (own work).



Sum of active forces : $F_a = 216.62$ kN/m
 Sum of passive forces : $F_p = 426.49$ kN/m
 Sliding moment : $M_a = 2793.95$ kN m/m
 Resisting moment : $M_p = 5500.77$ kN m/m
 Factor of safety = 1.97 < 1.50
Slope stability ACCEPTABLE

Figure 8: Slip curves along with the obtained factor of safety (own work).

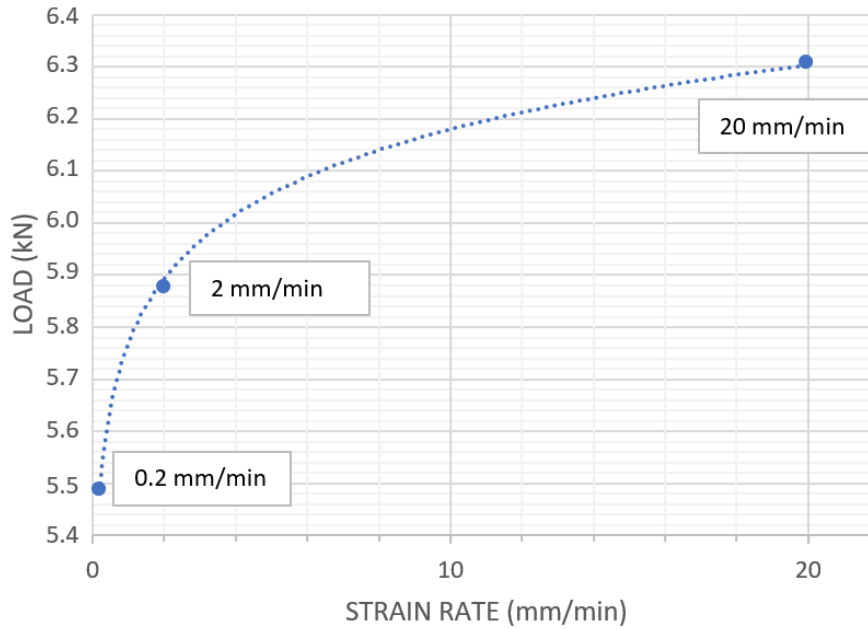


Figure 9: Increase in strength for woven geotextile with the strain rate (own work).

value obtained in case 2. In the presented situation, it may not be crucial since the factor of safety is greater than 1.5 in both cases. Nevertheless, it illustrates that the use of a material tested according to the standard results in higher values of the factor of safety in calculations. In a situation where the factor of safety would be close to the allowable value, this would be of significant importance.

6 Discussion

There is no doubt that the results obtained in Section 4 indicate that the tensile strength of the geosynthetic subjected to testing is dependent on the strain rate. This is clearly visible in Fig. 9, which depicts the relationship between the maximum load and the strain rate in individual series. The obtained results (Fig. 5) fit perfectly with the isochronous concept discussed in Section 1.

The obtained long-term strength results, according to Equation 5, are appropriately reduced using reduction factors, including the factor defining creep as a destructive process. This approach does not assume that the strength value of the geosynthetic after creep can reach the level it would have achieved without creep. In the first section, it was indicated that such a phenomenon occurs during the stretching of geosynthetics. Therefore, the properties of geosynthetics can be determined experimentally each time.

Based on the conducted research, analysis, and calculations, the influence of the woven geotextile on the stability of the given slope was examined. The initial factor of safety for the unreinforced slope was $F = 1.35$, which increased to $F = 2.08$ after using four layers of woven geotextile, whose parameters were obtained based on the tensile test results at a speed of 20 mm/min. In the next case, the results of reinforcement using the same embankment with geotextile defined based on the tensile test results at a speed of 0.2 mm/min were presented. The obtained factor of safety in this case was $F = 1.97$. Due to the strain rate, the material parameters in the third case were lower, resulting in a decrease in the factor of safety. The factor of safety results obtained from the program reflect the strength parameter results obtained from the test. The obtained results are closely related to the properties of the material in the PP geotextile. The change in strain rate highlights the fact that these are interconnected and entangled particle chains. Rapid stretching causes the chains to tighten rather than straighten, which is reflected in the apparent increase in strength. Slow stretching allows the chains to unravel, which reduces the strength while increasing elongation. Such changes must be reflected in the factor of safety results. The GEO5 software, when calculating the factor of safety, requires not only the soil properties but also the tensile strength parameters of the reinforcement, including long- and short-term strength as well as reduction factors. Therefore, these variables,

by reducing their values, determine the lower factor of safety results. The conducted study and calculations may be helpful; however, it is important to remember that despite using GEO5 for the calculations, the factor of safety results are only theoretical. While this study confirms the behavior of PP geotextiles under different strain rates, and the program's calculations indicate changes in the factor of safety, the software relies on data input by the user, making the results easily subject to manipulation. This study did not focus on temperature or the proper selection of soil. The behavior of geosynthetics will vary depending on these variables. Strain rate has a significant impact on strength parameters, but in reality, the strain rate is variable, meaning the material's deformation will also vary. To make the study fully comprehensive, it would be necessary to expand the range of variables while simultaneously limiting the possibility of data manipulation. Both the theoretical and calculation sections highlighted different methods for obtaining the tensile strength parameters of geotextiles depending on strain rate. Complementing this process with triaxial tests, large-scale tests, and more advanced computational methods could contribute to the creation of a database of soils and materials that work best together, ensuring that both during construction and operation, structures are protected by selecting the optimal reinforcement.

7 Conclusion

The research results, analysis, and calculations have practical implications for geotechnical engineers, designers, and practitioners. Understanding the properties of woven PP geotextiles and their role in soil reinforcement enables optimal design and construction, enhancing infrastructure safety and reducing the risk of slope failures and damage. The study also sheds light on the relationship between strain rate and the strength parameters of geotextiles, contributing to a better understanding of their behavior under varying loading conditions. The main conclusions drawn from this article are as follows:

1. The strength parameters of geosynthetics depend on the strain rate. Simply, the slower the geosynthetic is stretched, the lower its strength, while elongation increases.
2. The testing method of geosynthetics affects the results in the design phase of variable constructions.
3. Standard computational procedures assume the correctness of the isochronous concept, leading to

underestimated strength results for geosynthetic materials.

4. To make the results more reliable, it is necessary to expand it to include large-scale tests.
5. Future research should take a holistic approach, incorporating variables such as temperature, water condition variability, duration of reinforcement loading, and creep at once to get the closest to *in situ* condition.

References

- [1] Agrawal B. J., Geotextile its application to civil engineering- overview, Geotextile, India 2011.
- [2] Allen T.M., R. J., Soil Reinforcement Loads in Geosynthetic Walls at Working Stress Conditions, Geosynthetics International Volume 9 Issue 5-6, January 2002, pp. 525-566.
- [3] Benjamim C.V.S. ,Bueno B.S. , Zornberg J.G., Field monitoring evaluation of geotextile-reinforced soil-retaining walls. Geosynth. Int., 14 (2) (2007), pp. 100-118.
- [4] Bishop A.W., The use of the slip circle in the stability analysis of slopes. Géotechnique, 1955, 5(1): 7–17
- [5] Dąbrowska J., Kiersnowska A., Zięba Z., Trach Y., Sustainability of Geosynthetics-Based Solutions, (2023) *Environments - MDPI*, 10 (4), art. no. 64.
- [6] Dobrzański L.A. Podstawy nauki o materiałach i metaloznawstwo. Wydawnictwa Naukowo-Techniczne, Warsaw 2002.
- [7] Duszyńska A., Sikora Z., Dobór wyrobów geosyntetycznych do zbrojenia gruntu. Inżynieria Morska i Geotechnika, 5/2014.
- [8] EBGeo, Recommendations for 3-Design and Analysis of Earth Structures using Geosynthetic Reinforcements. Ernst & Sohn Verlag, Berlin, 2011.
- [9] EN ISO 10318-1:2015/Amd 1:201810318:2015 Geosynthetics – Part 1: Terms and Definitions.
- [10] EN ISO 10319:2015 Geosynthetics – Wide-width tensile test.
- [11] EN ISO 9862:2007 Geosynthetics – Sampling and preparation of test specimens.
- [12] Greenwood J.H., The effect of installation damage on the long-term design strength of a reinforcing geosynthetic. Geosynth Int. 2002, 9(3):247–258.
- [13] Greenwood, J. H., Designing to residual strength of geosynthetics instead of stress-rupture. Geosynthetics International, 4, No. 1, 1–10, 1998.
- [14] Greenwood, J.H., Schroeder, H.F., Voskamp, W., Durability of Geosynthetics; Stichting Curent: Gouda, The Netherlands; CUR: Rotterdam, The Netherlands, 2012.
- [15] Hassan, W., Alshameri, B., Nawaz, M.N. et al. Experimental study on shear strength behavior and numerical study on geosynthetic-reinforced cohesive soil slope. *Innov. Infrastruct. Solut.* 7, 349 (2022).
- [16] Hassan, W., Farooq, K., Hassan, M., Alshameri, B., Shahzad, A., Nawaz, M.N., Azab, M. Experimental investigation of mechanical behavior of geosynthetics in different soil plasticity indexes, *Transportation Geotechnics*, Volume 39,

- 2023, 100935, ISSN 2214-3912. <https://doi.org/10.1016/j.trgeo.2023.100935>.
- [17] Hirakawa D., Kongkitkul W., Tatsuoka F., Uchimura T., Time-dependent stress–strain behavior due to viscous properties of geogrid reinforcement. *Geosynthetics International*, 10, No. 6, 2003.
- [18] Hirakawa D., Uchimura T., Shibata Y. and Tatsuoka F., Time-dependent deformation of geosynthetics and geosynthetic-reinforced soil structures. *Geosynthetics - 7 ICG - Delmas, Gourc & Girard* 2002.
- [19] Hsuan et al., Long-term performance and lifetime prediction of geosynthetics, *EuroGeo4 Keynote Paper*, p. 1-40, 2008.
- [20] Ingold T.S., *The Geotextiles and Geomembranes Manual*, Elsevier Science Publishers Ltd., Oxford, United Kingdom, 610 p. 1994.
- [21] Instytut Techniki Budowlanej. Projektowanie konstrukcji oporowych, stromych skarp i nasypów z gruntu zbrojonego geosyntetykami. Instrukcje, Wytyczne, Poradniki nr 429/2008.
- [22] Janbu, N., Slope stability computations. In *Embankment Dam Engineering, Casagrande Memorial Volume*. Edited by E. Hirschfield and S. Poulos, 1973 pp. 47–86. Wiley, New York.
- [23] Kiersnowska A., Koda E., Fabianowski W. Kawalec J., Effect of the impact of chemical and environmental factors on the durability of the high density polyethylene (HDPE) geogrid in a sanitary landfill. *Appl. Sci.* 7, 22, 2017.
- [24] Kiersnowska A., Stępień S., Research the effect of temperature changes on strain and strength of woven geotextile. *Włókno Odzież, Skóra*, 2014, 68, 25-29.
- [25] Kiersnowska, A., Fabianowski, W., Koda, E. The influence of the accelerated aging conditions on the properties of polyolefin geogrids used for landfill slope reinforcement. *Polymers*, 12 (9), art. no. 1874, 2020.
- [26] Koda E., Kiersnowska A., Kawalec J., and Osiński P. Landfill slope stability improvement incorporating reinforcements in reclamation process applying observational method. *Applied Sciences*, 10(5), 1572, 2020.
- [27] Koda E., Osiński P., Kiersnowska A., Kawalec J., Stabilizacja georusztem heksagonalnym podłoża pod trasę narciarską na składowisku, *Acta Sci. Pol. Architectura* 15(4), 2016.
- [28] Koerner R.M., *Designing with Geosynthetics - 6th Edition*. Vol. 1(1), USA, 2012.
- [29] Kongkitkul W., Chantachot T. and Tatsuoka F. Simulation of geosynthetic load–strain–time behaviour by the non-linear three-component model. *Geosynthetics International*, 2014, 21, No. 4.
- [30] Lee W.F., Lin S.S., Chang D.T.T, Lin S.Y.: Influence of strain rate on geosynthetic reinforcement properties, *Geosynthetics - 7 ICG - Delmas, Gourc & Girard* 2002.
- [31] Miskowska A., Stępień S., Jasko A., Koda E., Wpływ temperatury na parametry wytrzymałościowe geotkaniny wykorzystywanej do budowy konstrukcji oporowej na składowisku, Warszawa 2015.
- [32] Morgenstern N.R. and Price V., The analysis of the stability of general slip surface. *Géotechnique*, 15(1): 79–93, 1965.
- [33] Paula A.M., Pinho-Lopes M., Constitutive Modelling of Short-Term Tensile Response of Geotextile Subjected to Mechanical and Abrasion Damages. *Int. J. of Geosynth. and Ground Eng.* 7, 67, 2021.
- [34] Sawicki A. and Kazmierowicz-Frankowska K., Influence of Strain Rate on the Load-Strain Characteristics of Geosynthetics, *Geosynthetics International*, Vol. 9, No. 1, pp. 1-19, 2002
- [35] Shukla S. K, Yin J., *Fundamentals of geosynthetic engineering*, CRC Press, 2006.
- [36] Shukla S. K., *An introduction to Geosynthetic Engineering*, CRC Press, 2017.
- [37] Stein R.S., Powers J., *Topics in polimer physics*. London Imperial College Press 2006.
- [38] Stępień S., Szymański A. 2015. Influence of strain rate on tensile strength of woven geotextile in the selected range of temperature. *Studia Geotechnica et Mechanica*, Vol. 37(2), 57-60.
- [39] Stępień S., Szymański A., Influence of Strain Rate on Tensile Strength of Woven Geotextile in the Selected Range of Temperature, *Studia Geotechnica et Mechanica*, Vol. 37, No. 2, 2015.
- [40] Wysokiński L., Kotlicki W., Projektowanie konstrukcji oporowych, stromych skarp i nasypów z gruntu zbrojonego geosyntetykami. Instrukcje, Wytyczne, Poradniki 429/2008, Warszawa 2008.
- [41] Yang G., Zhang B., Zhou P. Lv, Q., Behaviour of geogrid reinforced soil retaining wall with concrete-rigid facing, *Geotext. Geomembranes*, 27 (5) (2009), pp. 350-356.